



Magnetic dipole moments of the hidden-charm pentaquark states: $P_c(4440)$, $P_c(4457)$ and $P_{cs}(4459)$

Ulaş Özdem^a

Health Services Vocational School of Higher Education, Istanbul Aydın University, Sefakoy-Kucukcekmece, 34295 Istanbul, Turkey

Received: 3 February 2021 / Accepted: 19 March 2021 / Published online: 2 April 2021
© The Author(s) 2021

Abstract In this work, we employ the light-cone QCD sum rule to calculate the magnetic dipole moments of the $P_c(4440)$, $P_c(4457)$ and $P_{cs}(4459)$ pentaquark states by considering them as the diquark–diquark–antiquark and molecular pictures with quantum numbers $J^P = \frac{3}{2}^-$, $J^P = \frac{1}{2}^-$ and $J^P = \frac{1}{2}^-$, respectively. In the analyses, we use the diquark–diquark–antiquark and molecular form of interpolating currents, and photon distribution amplitudes to obtain the magnetic dipole moment of pentaquark states. Theoretical examinations on magnetic dipole moments of the hidden-charm pentaquark states, are essential as their results can help us better figure out their substructure and the dynamics of the QCD as the theory of the strong interaction. As a by product, we extract the electric quadrupole and magnetic octupole moments of the $P_c(4440)$ pentaquark. These values show a non-spherical charge distribution.

1 Motivation

With the experimental discovery of the exotic X(3872) state, i.e., state that cannot be interpreted by the conventional meson or baryon picture, a new era began in high energy physics. Since the discovery of this state, numerous exotic states have been added to the family of particles that have been experimentally reported. Study of exotic particles that are composed of tetraquark, pentaquark or hybrid states is among the most attractive subjects of the hadron physics. Experimental data collected with various collaborations in recent years and theoretical developments obtained in different theoretical models form the field of rapidly growing exotic studies [1–11].

In 2019, LHCb collaboration reported three new narrow pentaquark states [12] as

$$\begin{aligned} P_c(4312) : M &= 4311.9 \pm 0.7_{-0.6}^{+6.8} \text{ MeV}, \\ \Gamma &= 9.80 \pm 2.7_{-4.5}^{+3.7} \text{ MeV}, \\ P_c(4440) : M &= 4440.3 \pm 1.3_{-4.7}^{+4.1} \text{ MeV}, \\ \Gamma &= 20.6 \pm 4.9_{-10.1}^{+8.7} \text{ MeV}, \\ P_c(4457) : M &= 4457.3 \pm 0.6_{-1.7}^{+4.1} \text{ MeV}, \\ \Gamma &= 6.40 \pm 2.0_{-1.9}^{+5.7} \text{ MeV}. \end{aligned}$$

Very recently, the LHCb Collaboration reported a pentaquark state with strangeness, $P_{cs}(4459)$, in the invariant mass spectrum of $J/\psi \Lambda$ in the $\Xi_b^0 \rightarrow J/\psi \Lambda K^-$ decay [13]:

$$\begin{aligned} P_{cs}(4459) : M &= 4458.8 \pm 2.7_{-1.1}^{+4.7} \text{ MeV}, \\ \Gamma &= 17.3 \pm 6.5_{-5.7}^{+8.0} \text{ MeV}. \end{aligned} \quad (1)$$

But, spin and parity of the $P_{cs}(4459)$ state have not been determined yet. As regards to their decay products, one can easily conclude that these newly discovered four states consist of at least five quarks, $\bar{c}uud$ or $\bar{c}uds$, therefore they are perfect candidates of hidden-charm pentaquark states. After the experimental discovery several phenomenological models have been adopted to calculate the spectroscopic parameters, decays and production mechanisms of the pentaquarks, like the QCD sum rule, the meson-exchange model, the quark delocalization model, and so on [14–55]. However, the substructure of these states are not determined yet. In other words, in order to understand the internal structure and nature of these particles, different properties should be studied besides their decay channels and spectroscopic properties. For instance, investigating their electromagnetic form factors may provide important insights on this point.

Electromagnetic form factors or multi-pole moments of hadrons are important parameters in study of their electromagnetic structure, and also they can ensure important knowledge about the dynamics of the QCD at low

^ae-mail: ulasozdem@aydin.edu.tr (corresponding author)

energy region. Electromagnetic multi-pole moments, especially magnetic dipole moment, are also a crucial part in the calculation of J/ψ photo-production cross sections, which can provide an independent analysis of the hidden-charm pentaquark states. Investigating electromagnetic features of exotic resonances is relatively new topic. However, in the literature there are a few studies where the electromagnetic properties of the hidden-charm pentaquark states are investigated [56–60]. In Ref. [56], the magnetic dipole moment of the hidden-charm pentaquark states have been extracted in the diquark–diquark–antiquark, diquark–triquark and molecular configuration with $J^P = \frac{1}{2}^\pm, \frac{3}{2}^\pm, \frac{5}{2}^\pm$ and $\frac{7}{2}^+$ quantum numbers in the different color-flavor structure. In Ref. [57], the magnetic dipole, electric quadrupole and magnetic octupole moments of the $P_c(4380)$ pentaquark with $J^P = \frac{3}{2}^-$ quantum numbers have been obtained in the diquark–diquark–antiquark and molecular pictures in the framework of the light-cone QCD sum rule (LCSR). In Ref. [58], they acquired the ground state of hidden-charm pentaquarks with $J^P = \frac{3}{2}^-$ quantum numbers and their associated magnetic dipole moments and electromagnetic couplings, of interest to pentaquark photoproduction experiments in the framework of the constituent quark model. In Ref. [59], the magnetic dipole moment of the $P_c(4312)$ pentaquark state have been extracted in the molecular and diquark–diquark–antiquark pictures via the LCSR with $J^P = \frac{1}{2}^-$ quantum numbers. In Ref. [60], they achieved the magnetic dipole moment of the $P_c(4312)$ pentaquark state in the $\Sigma_c \bar{D}$ molecular picture by means of the QCD sum rule (QCDSR) in the external weak electromagnetic field.

In this study, the magnetic dipole moments of the pentaquark states $P_c(4440)$, $P_c(4457)$ and $P_{cs}(4459)$ (hereafter we will show these states as P_{c1} , P_{c2} and P_{cs} , respectively) are obtained by employing the diquark–diquark–antiquark and molecular interpolating currents within the LCSR.

The LCSR is a powerful tool to obtain qualitative and quantitative information about hadron properties. In this method, hadrons are analytically studied by matching their behaviors at high and low energies. This matching provides characteristic properties of hadrons from QCD. The information obtained by LCSR has been used as an input to other theoretical and experimental approaches for a long time [61–63].

The rest of paper is structured as follows. In Sect. 2, the method used for the calculations are described. In Sect. 3, we carry out numerical analysis of the acquired LCSR for the magnetic dipole moment of pentaquark states. The explicit expressions of the magnetic moment of the P_{c1} pentaquark in the diquark–diquark–antiquark picture is presented in Appendix A.

2 Magnetic dipole moments of the pentaquark states via LCSR

In this section, we briefly introduce the LCSR method used to extract the magnetic dipole moments of the P_{c1} , P_{c2} and P_{cs} pentaquark states. In order to obtain the magnetic dipole moment of the corresponding states with the QCD sum rule method, we begin by writing the correlation function suitable for the calculations. This correlation function is obtained in two representations which are called hadronic and QCD representations. The LCSR for the physical quantities are obtained from the matches of the coefficients of the same Lorentz structures achieved on both representations with the help of the quark-duality ansatz.

2.1 Formalism of the P_{c2} and P_{cs} states

The current correlation function for the P_{c2} and P_{cs} pentaquark states is written as

$$\Pi(p, q) = i \int d^4x e^{ip \cdot x} \langle 0 | \mathcal{T} \{ J_{P_{c2(cs)}}(x) \bar{J}_{P_{c2(cs)}}(0) \} | 0 \rangle_\gamma, \tag{2}$$

where $J_{P_{c2(cs)}}(x)$ is the interpolating current of P_{c2} or P_{cs} pentaquark state. In the diquark–diquark–antiquark and molecular pictures with quantum number $J^P = \frac{1}{2}^-$, they are written as

$$\begin{aligned} J_{P_{c2}}^{Di}(x) &= \varepsilon^{abc} \varepsilon^{ade} \varepsilon^{bfg} [u_d^T(x) C \gamma_5 d_e(x) u_f^T(x) \\ &\quad C \gamma_\mu c_g(x) \gamma_5 \gamma^\mu C \bar{c}_c^T(x)], \\ J_{P_{c2}}^{Mol}(x) &= [\bar{c}_d(x) \gamma_\mu u_d(x)] \gamma^\mu \gamma_5 [\varepsilon^{abc} u_a^T(x) \\ &\quad C \gamma_\nu d_b(x) \gamma^\nu \gamma_5 c_c(x)], \end{aligned} \tag{3}$$

$$\begin{aligned} J_{P_{cs}}^{Di}(x) &= \varepsilon^{abc} \varepsilon^{ade} \varepsilon^{bfg} [u_d^T(x) C \gamma_5 d_e(x) s_f^T(x) \\ &\quad C \gamma_5 c_g(x) C \bar{c}_c^T(x)], \\ J_{P_{cs}}^{Mol}(x) &= [\bar{c}_d(x) \gamma_\mu u_d(x)] \gamma^\mu \gamma_5 [\varepsilon^{abc} d_a^T(x) \\ &\quad C \gamma_5 s_b(x) c_c(x)], \end{aligned} \tag{4}$$

where C is the charge conjugation matrix; and a, b, \dots are color indices.

As we mentioned at the beginning of this section, in LCSR studies we need to evaluate the correlation function at both hadron and quark-gluon degrees of freedom. At the hadron level, we embedding a complete set of intermediate pentaquark states into the correlation function to acquire the hadronic representation, and isolate the ground state pentaquark states, and get the results:

$$\begin{aligned} \Pi^{Had}(p, q) &= \frac{\langle 0 | J_{P_{c2(cs)}} | P_{c2(cs)}(p, s) \rangle}{[p^2 - m_{P_{c2(cs)}}^2]} \\ &\times \langle P_{c2(cs)}(p, s) | P_{c2(cs)}(p + q, s) \rangle_\gamma \\ &\times \frac{\langle P_{c2(cs)}(p + q, s) | \bar{J}_{P_{c2(cs)}} | 0 \rangle}{[(p + q)^2 - m_{P_{c2(cs)}}^2]} + \dots \end{aligned} \quad (5)$$

The matrix element $\langle P_{c2(cs)}(p, s) | P_{c2(cs)}(p + q, s) \rangle_\gamma$ entering Eq. (5) can be parameterized in terms of Lorentz invariant form factors as follows:

$$\begin{aligned} \langle P_{c2(cs)}(p, s) | P_{c2(cs)}(p + q, s) \rangle_\gamma &= \varepsilon^\mu \bar{u}(p, s) \left[[f_1(q^2) + f_2(q^2)] \gamma_\mu \right. \\ &\left. + f_2(q^2) \frac{(2p + q)_\mu}{2m_{P_{c2(cs)}}} \right] u(p + q, s), \end{aligned} \quad (6)$$

where ε and q are the polarization vector and momentum of the photon, respectively.

Substituting Eq. (6) in Eq. (5) for hadronic side we get

$$\begin{aligned} \Pi^{Had}(p, q) &= \lambda_{P_{c2(cs)}}^2 \gamma_5 \\ &\frac{(\not{p} + m_{P_{c2(cs)}})}{[p^2 - m_{P_{c2(cs)}}^2]} \varepsilon^\mu \left[[f_1(q^2) + f_2(q^2)] \gamma_\mu \right. \\ &\left. + f_2(q^2) \frac{(2p + q)_\mu}{2m_{P_{c2(cs)}}} \right] \gamma_5 \frac{(\not{p} + \not{q} + m_{P_{c2(cs)}})}{[(p + q)^2 - m_{P_{c2(cs)}}^2]}, \end{aligned} \quad (7)$$

with $\langle 0 | J_{P_{c2(cs)}} | P_{c2(cs)}(p, s) \rangle = \lambda_{P_{c2(cs)}} \gamma_5 u(p, s)$. The Lorentz invariant form factors $f_1(q^2)$ and $f_2(q^2)$ are related to the magnetic form factor by the relation,

$$G_M(q^2) = f_1(q^2) + f_2(q^2). \quad (8)$$

At $q^2 = 0$, the magnetic form factor is acquired associated with the functions $f_1(q^2)$ and $f_2(q^2)$ as:

$$G_M(0) = f_1(0) + f_2(0). \quad (9)$$

The magnetic dipole moment, $\mu_{P_{c2(cs)}}$, is defined in the following way:

$$\mu_{P_{c2(cs)}} = G_M(0) \frac{e}{2m_{P_{c2(cs)}}}. \quad (10)$$

We observe from Eq. (7) that the correlation function contains many structures, any of them can be selected in obtaining magnetic dipole moment of the $P_{c2(cs)}$ pentaquark, and thus we decide on the structure $\not{\varepsilon}\not{q}$. As a result, the correlation

function can be expressed with regards to the magnetic dipole moment of $P_{c2(cs)}$ pentaquark as,

$$\Pi^{Had}(p, q) = \frac{\lambda_{P_{c2(cs)}}^2 m_{P_{c2(cs)}}}{[(p + q)^2 - m_{P_{c2(cs)}}^2]} \mu_{P_{c2(cs)}} \frac{1}{[p^2 - m_{P_{c2(cs)}}^2]}. \quad (11)$$

At the QCD level, we contract the relevant quark fields in the correlation function with the help of the Wick's theorem,

$$\begin{aligned} \Pi_{P_{c2}}^{QCD-Di}(p, q) &= i \varepsilon^{abc} \varepsilon^{a'b'c'} \varepsilon^{ade} \varepsilon^{a'd'e'} \varepsilon^{bfg} \varepsilon^{b'f'g'} \\ &\times \int d^4x e^{ip \cdot x} \langle 0 | \\ &\times \left\{ Tr \left[\gamma_5 S_d^{ee'}(x) \gamma_5 \tilde{S}_u^{dd'}(x) \right] \right. \\ &\times Tr \left[\gamma_\mu S_c^{gg'}(x) \gamma_\nu \tilde{S}_u^{ff'}(x) \right] \\ &\left. - Tr \left[\gamma_5 S_d^{ee'}(x) \gamma_5 \tilde{S}_u^{fd'}(x) \gamma_\mu S_c^{gg'}(x) \gamma_\nu \tilde{S}_u^{df'}(x) \right] \right\} \\ &\times \left(\gamma_5 \gamma^\mu S_c^{c'c}(-x) \gamma^\nu \gamma_5 \right) | 0 \rangle_\gamma, \end{aligned} \quad (12)$$

$$\begin{aligned} \Pi_{P_{c2}}^{QCD-Mol}(p, q) &= i \varepsilon^{abc} \varepsilon^{a'b'c'} \\ &\times \int d^4x e^{ip \cdot x} \langle 0 | Tr \left[\gamma_\mu S_u^{dd'}(x) \gamma_\alpha S_c^{d'd}(-x) \right] \\ &\times Tr \left[\gamma_\nu S_d^{bb'}(x) \gamma_\beta \tilde{S}_u^{aa'}(x) \right] \\ &\left. - Tr \left[\gamma_\mu S_u^{da'}(x) \gamma_\beta \tilde{S}_d^{bb'}(x) \right] \right. \\ &\times Tr \left[\gamma_\nu S_u^{ad'}(x) \gamma_\alpha S_c^{d'd}(-x) \right] \left. \right\} \\ &\times \left(\gamma^\mu \gamma^\nu S_c^{cc'}(x) \gamma^\alpha \gamma^\beta \right) | 0 \rangle_\gamma, \end{aligned} \quad (13)$$

$$\begin{aligned} \Pi_{P_{cs}}^{QCD-Di}(p, q) &= -i \varepsilon^{abc} \varepsilon^{a'b'c'} \varepsilon^{ade} \varepsilon^{a'd'e'} \varepsilon^{bfg} \varepsilon^{b'f'g'} \\ &\times \int d^4x e^{ip \cdot x} \\ &\times \langle 0 | Tr \left[\gamma_5 S_d^{ee'}(x) \gamma_5 \tilde{S}_u^{dd'}(x) \right] \\ &\times Tr \left[\gamma_5 S_c^{gg'}(x) \gamma_5 \tilde{S}_s^{ff'}(x) \right] \tilde{S}_c^{c'c}(-x) | 0 \rangle_\gamma, \end{aligned} \quad (14)$$

$$\begin{aligned} \Pi_{P_{cs}}^{QCD-Mol}(p, q) &= -i \varepsilon^{abc} \varepsilon^{a'b'c'} \int d^4x e^{ip \cdot x} \\ &\times \langle 0 | Tr \left[\gamma_\nu S_u^{dd'}(x) \gamma_\mu S_c^{d'd}(-x) \right] \\ &\times Tr \left[\gamma^\nu \tilde{S}_s^{bb'}(x) \gamma^\mu S_d^{aa'}(x) \right] S_c^{c'c}(x) | 0 \rangle_\gamma, \end{aligned} \quad (15)$$

where

$$\tilde{S}_{c(q)}^{ij}(x) = C S_{c(q)}^{ijT}(x) C,$$

with $S_{q(c)}(x)$ being the full light and charm quark propagators. The relevant propagators are given as [64]

$$S_q(x) = i \frac{\not{x}}{2\pi^2 x^4} - \frac{\bar{q}q}{12} \left(1 - i \frac{m_q \not{x}}{4}\right) - \frac{\bar{q}q}{192} m_0^2 x^2 \left(1 - i \frac{m_q \not{x}}{6}\right) - \frac{ig_s}{32\pi^2 x^2} G^{\mu\nu}(x) [k\sigma_{\mu\nu} + \sigma_{\mu\nu}k], \tag{16}$$

$$S_c(x) = \frac{m_c^2}{4\pi^2} \left[\frac{K_1(m_c \sqrt{-x^2})}{\sqrt{-x^2}} + i \frac{\not{x} K_2(m_c \sqrt{-x^2})}{(\sqrt{-x^2})^2} \right] - \frac{g_s m_c}{16\pi^2} \int_0^1 dv G^{\mu\nu}(vx) [(\sigma_{\mu\nu} \not{x} + \not{x} \sigma_{\mu\nu}) \times \frac{K_1(m_c \sqrt{-x^2})}{\sqrt{-x^2}} + 2\sigma_{\mu\nu} K_0(m_c \sqrt{-x^2})], \tag{17}$$

where K_i are modified the second kind Bessel functions and $G^{\mu\nu}$ is the gluon field strength tensor.

The QCD representation of the correlation function can be obtained with the help of photon distribution amplitudes (DAs) according to quark-gluon properties and after performing the Fourier transform to transfer the calculations to the momentum space.

As a final step, by applying the double Borel transform on the variables $-p^2$ and $(p+q)^2$ and choosing the coefficients of the same Lorentz structures in both QCD and hadronic representations and matching them employing the quark-hadron duality approach, we obtain the desired LCSR for magnetic dipole moments of P_{c2} and P_{cs} states:

$$\mu_{P_{c2}}^{Di} \lambda_{P_{c2}}^{2-Di} m_{P_{c2}} = e \frac{m_{P_{c2}}^2}{M^2} \Delta_1^{QCD}, \tag{18}$$

$$\mu_{P_{c2}}^{Mol} \lambda_{P_{c2}}^{2-Mol} m_{P_{c2}} = e \frac{m_{P_{c2}}^2}{M^2} \Delta_2^{QCD}, \tag{19}$$

$$\mu_{P_{cs}}^{Di} \lambda_{P_{cs}}^{2-Di} m_{P_{cs}} = e \frac{m_{P_{cs}}^2}{M^2} \Delta_3^{QCD}. \tag{20}$$

$$\mu_{P_{cs}}^{Di} \lambda_{P_{cs}}^{2-Mol} m_{P_{cs}} = e \frac{m_{P_{cs}}^2}{M^2} \Delta_4^{QCD}. \tag{21}$$

The Δ_1^{QCD} , Δ_2^{QCD} , Δ_3^{QCD} and Δ_4^{QCD} functions are quite lengthy, therefore the explicit expression of this function are not presented here.

2.2 Formalism of the P_{c1} state

In this subsection we derive the LCSR for the magnetic dipole moment of the P_{c1} pentaquark state. For this purpose, we

consider following correlation function,

$$\Pi_{\mu\nu}(p, q) = i \int d^4x e^{ip \cdot x} \langle 0 | T \{ J_{\mu}^{P_{c1}}(x) \bar{J}_{\nu}^{P_{c1}}(0) \} | 0 \rangle_{\gamma}, \tag{22}$$

where $J_{\mu}^{P_{c1}}$ is the interpolating current of P_{c1} pentaquark with $J^P = \frac{3}{2}^-$ quantum numbers. In the diquark–diquark–antiquark and molecular pictures, it is given as

$$J_{\mu}^{P_{c1-Di}}(x) = \varepsilon^{abc} \varepsilon^{ade} \varepsilon^{bfg} [u_d^T(x) C \gamma_5 d_e(x) u_f^T(x) C \gamma_{\mu} c_g(x) C \bar{c}_c^T(x)],$$

$$J_{\mu}^{P_{c1-Mol}}(x) = [\bar{c}_d(x) \gamma_{\mu} u_d(x)] [\varepsilon^{abc} u_a^T(x) C \gamma_{\nu} d_b(x) \gamma^{\nu} \gamma_5 c_c(x)] \tag{23}$$

The hadronic side of the correlation function is written as,

$$\Pi_{\mu\nu}^{Had}(p, q) = \frac{\langle 0 | J_{\mu}^{P_{c1}} | P_{c1}(p) \rangle}{[p^2 - m_{P_{c1}}^2]} \times \langle P_{c1}(p) | P_{c1}(p+q) \rangle_{\gamma} \times \frac{\langle P_{c1}(p+q) | \bar{J}_{\nu}^{P_{c1}} | 0 \rangle}{[(p+q)^2 - m_{P_{c1}}^2]} + \dots \tag{24}$$

The matrix element of the interpolating current between the vacuum and the P_{c1} pentaquark is defined as

$$\langle 0 | J_{\mu}^{P_{c1}}(0) | P_{c1}(p, s) \rangle = \lambda_{P_{c1}} u_{\mu}(p, s), \tag{25}$$

where $\lambda_{P_{c1}}$ is the residue P_{c1} pentaquark and $u_{\mu}(p, s)$ is the Rarita-Schwinger spinor.

The transition matrix element $\langle P_{c1}(p) | P_{c1}(p+q) \rangle_{\gamma}$ entering Eq. (24) can be parameterized in terms of four Lorentz invariant form factors as follows [65–68]:

$$\langle P_{c1}(p) | P_{c1}(p+q) \rangle_{\gamma} = -e \bar{u}_{\mu}(p) \left[F_1(q^2) g_{\mu\nu} \not{\epsilon} - \frac{1}{2m_{P_{c1}}} \left[F_2(q^2) g_{\mu\nu} + F_4(q^2) \frac{q_{\mu} q_{\nu}}{(2m_{P_{c1}})^2} \right] \not{\epsilon} \not{q} + F_3(q^2) \frac{1}{(2m_{P_{c1}})^2} q_{\mu} q_{\nu} \not{\epsilon} \right] u_{\nu}(p+q). \tag{26}$$

In principle, we can obtain the final expression of the hadronic side of the correlation function using the above equations, but we encounter two difficulties: not all Lorentz structures are independent and the correlation function also includes contributions of spin-1/2 and these undesirable contributions must be eliminated. To remove undesirable contributions coming from the spin-1/2 particles and obtain only independent structures in the correlation function, we apply the ordering for Dirac matrices as $\gamma_{\mu} \not{\epsilon} \not{q} \gamma_{\nu}$ and remove terms with γ_{μ} at the beginning, γ_{ν} at the end and those proportional to p_{μ} and p_{ν} [69]. As a result, using Eqs. (22)–(26)

the hadronic side take the form,

$$\begin{aligned} \Pi_{\mu\nu}^{Had}(p, q) = & \frac{\lambda_{P_{c1}}^2}{[(p+q)^2 - m_{P_{c1}}^2][p^2 - m_{P_{c1}}^2]} \left[g_{\mu\nu} \not{p} \not{q} F_1(q^2) \right. \\ & - m_{P_{c1}} g_{\mu\nu} \not{q} F_2(q^2) - \frac{F_3(q^2)}{4m_{P_{c1}}} q_\mu q_\nu \not{q} \\ & - \frac{F_4(q^2)}{4m_{P_{c1}}^3} (\varepsilon \cdot p) q_\mu q_\nu \not{q} \\ & \left. + \text{other independent structures} \right]. \end{aligned} \tag{27}$$

The final form of the hadronic side in terms of the selected structures in momentum space is:

$$\Pi_{\mu\nu}^{Had}(p, q) = \Pi_1^{Had} g_{\mu\nu} \not{p} \not{q} + \Pi_2^{Had} g_{\mu\nu} \not{q} + \dots, \tag{28}$$

where Π_1^{Had} and Π_2^{Had} are functions of the form factors $F_1(q^2)$ and $F_2(q^2)$, respectively; and other independent structures is represented by dots.

The magnetic, $G_M(q^2)$, form factor is defined in terms of the form factors $F_i(q^2)$ in the following way [65–68]:

$$\begin{aligned} G_M(q^2) = & [F_1(q^2) + F_2(q^2)](1 + \frac{4}{5}\tau) \\ & - \frac{2}{5}[F_3(q^2) + F_4(q^2)]\tau(1 + \tau), \end{aligned} \tag{29}$$

where $\tau = -\frac{q^2}{4m_{P_{c1}}^2}$. At $q^2 = 0$, the magnetic dipole moment is obtained in terms of the functions $F_1(0)$ and $F_2(0)$ as:

$$G_M(0) = F_1(0) + F_2(0). \tag{30}$$

The magnetic dipole moment, ($\mu_{P_{c1}}$), is defined in the following way:

$$\mu_{P_{c1}} = \frac{e}{2m_{P_{c1}}} G_M(0). \tag{31}$$

The next step is to calculate the correlation function in Eq. (22) in terms of quark-gluon parameters. When we apply the same procedures as in the previous subsection, we get the following result:

$$\begin{aligned} \Pi_{\mu\nu}^{QCD-Di}(p, q) = & i \varepsilon^{abc} \varepsilon^{a'b'c'} \varepsilon^{ade} \varepsilon^{a'd'e'} \varepsilon^{bfg} \varepsilon^{b'f'g'} \\ & \times \int d^4x e^{ip \cdot x} \langle 0 | \\ & \times \left\{ Tr \left[\gamma_5 S_d^{ee'}(x) \gamma_5 \tilde{S}_u^{dd'}(x) \right] \right. \\ & \times Tr \left[\gamma_\mu S_c^{gg'}(x) \gamma_\nu \tilde{S}_u^{ff'}(x) \right] \tilde{S}_c^{c'c}(-x) \\ & - Tr \left[\gamma_5 S_d^{ee'}(x) \gamma_5 \tilde{S}_u^{fd'}(x) \gamma_\mu S_c^{gg'}(x) \gamma_\nu \tilde{S}_u^{df'}(x) \right] \\ & \left. \times \tilde{S}_c^{c'c}(-x) \right\} |0\rangle_\gamma, \end{aligned} \tag{32}$$

$$\begin{aligned} \Pi_{\mu\nu}^{QCD-Mol}(p, q) = & -i \varepsilon^{abc} \varepsilon^{a'b'c'} \\ & \times \int d^4x e^{ip \cdot x} \langle 0 | \left\{ Tr \left[\gamma_\mu S_u^{dd'}(x) \gamma_\nu S_c^{d'd}(-x) \right] \right. \\ & \times Tr \left[\gamma_\beta \tilde{S}_u^{aa'}(x) \gamma_\alpha S_d^{bb'}(x) \right] \\ & - Tr \left[\gamma_\mu S_u^{dd'}(x) \gamma_\nu S_c^{d'd}(-x) \right] \\ & \left. \times Tr \left[\gamma_\beta \tilde{S}_u^{ba'}(x) \gamma_\alpha S_d^{ab'}(x) \right] \right\} \\ & \times \left(\gamma^\alpha \gamma_5 S_c^{cc'}(x) \gamma_5 \gamma^\beta \right) |0\rangle_\gamma. \end{aligned} \tag{33}$$

As a result, the QCD side of the correlation function in terms of the selected structures is obtained as

$$\Pi_{\mu\nu}^{QCD}(p, q) = \Pi_1^{QCD} g_{\mu\nu} \not{p} \not{q} + \Pi_2^{QCD} g_{\mu\nu} \not{q} + \dots \tag{34}$$

The following processes are applied as described in the previous subsection and magnetic dipole moment results are obtained in LCSR. The QCD and hadronic representations of the correlation function are then matched employing quark-duality assumption. By equating the coefficients of the structures $g_{\mu\nu} \not{p} \not{q}$ and $g_{\mu\nu} \not{q}$, respectively for the F_1 and F_2 we obtain sum rules for these two form factors. As a result, we get,

$$\Pi_{\mu\nu}^{Had}(p, q) = \Pi_{\mu\nu}^{QCD}(p, q). \tag{35}$$

The explicit expressions of the LCSR for the F_1^{Di} and F_2^{Di} are presented in the Appendix A. We are now ready to move on to numerical analysis.

3 Numerical analysis and discussions

This section is devoted to the numerical computations for the magnetic dipole moments of the P_{c1} , P_{c2} and P_{cs} pentaquark states. We use $m_u = m_d = 0$, $m_s = 96_{-4}^{+8}$ MeV, $m_c = 1.275 \pm 0.02$ GeV [70], $m_{P_{c1}} = 4440.3 \pm 1.3_{-4.7}^{+4.1}$ MeV, $m_{P_{c2}} = 4457.3 \pm 0.6_{-1.7}^{+4.1}$ MeV [12], $m_{P_{cs}} = 4458.8 \pm 2.7_{-1.1}^{+4.7}$ MeV [13], $f_{3\gamma} = -0.0039$ GeV² [71], $\langle \bar{u}u \rangle = \langle \bar{d}d \rangle = (-0.24 \pm 0.01)^3$ GeV³, $\langle \bar{s}s \rangle = 0.8 \langle \bar{u}u \rangle$ GeV³ [72], $m_0^2 = 0.8 \pm 0.1$ GeV² [72], $\langle g_s^2 G^2 \rangle = 0.88$ GeV⁴ [73], $\lambda_{P_{c1}}^{Di} = (1.44 \pm 0.23) \times 10^{-3}$ GeV⁶, $\lambda_{P_{c2}}^{Di} = (3.02 \pm 0.48) \times 10^{-3}$ GeV⁶ [28], $\lambda_{P_{cs}}^{Di} = (1.86 \pm 0.31) \times 10^{-3}$ GeV⁶ [53], $\lambda_{P_{c1}}^{Mol} = (1.15_{-0.18}^{+0.16}) \times 10^{-3}$ GeV⁶, $\lambda_{P_{c2}}^{Mol} = (2.24_{-0.34}^{+0.30}) \times 10^{-3}$ GeV⁶ [48] and $\lambda_{P_{cs}}^{Mol} = 1.13 \times 10^{-3}$ GeV⁶. Another set of main input parameters are the photon wavefunctions of different twists, entering the DAs. These wavefunctions are given in Ref. [71].

Except the above mentioned input parameters, the estimations for the magnetic dipole moments of pentaquark states

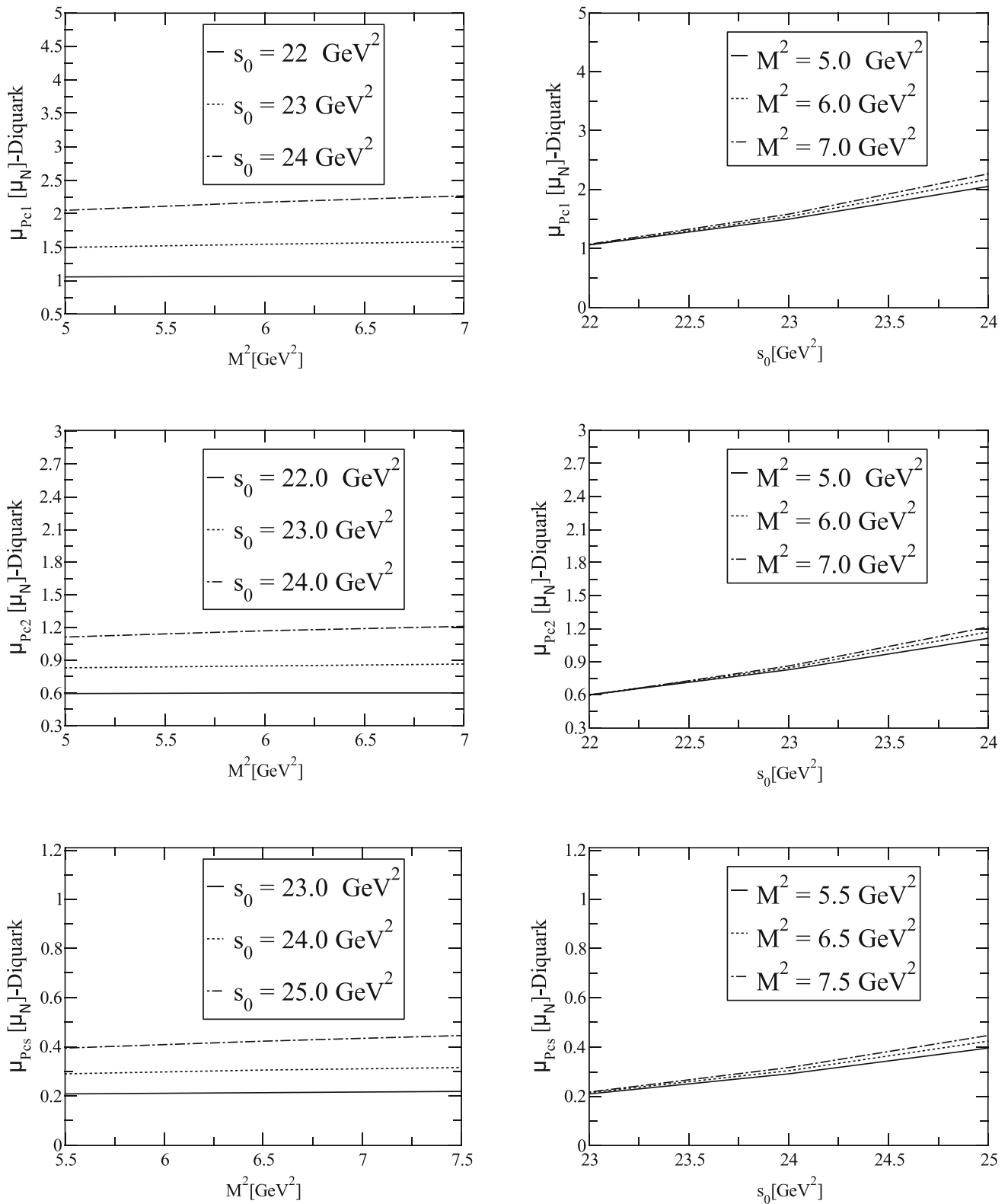


Fig. 1 Variations of the magnetic dipole moments of $\mu_{P_{c1}}$, $\mu_{P_{c2}}$ and $\mu_{P_{cs}}$ in diquark–diquark–antiquark picture with M^2 and s_0

depend on two auxiliary parameters: Borel mass parameter M^2 and continuum threshold s_0 . According to the philoso-

phy of the method used, the observables under examination should be weakly dependent on the variations of these aux-

Table 1 Results of the magnetic dipole moments (in units of μ_N) for the pentaquark states

Picture	$\mu_{P_{c1}}$	$\mu_{P_{c2}}$	$\mu_{P_{cs}}$
Diquark	$1.62^{+0.65}_{-0.57}$	$0.88^{+0.32}_{-0.29}$	$0.34^{+0.13}_{-0.11}$
Molecule	$3.49^{+1.49}_{-1.31}$	$2.78^{+0.94}_{-0.83}$	$1.75^{+0.64}_{-0.58}$

iliary parameters. The continuum threshold is considered to be the point where the excited states and continuum begin to contribute to the correlation function. The upper and lower bound of the Borel parameter is decided by demanding that both the contributions of the higher states and continuum are adequately suppressed and the contributions coming from higher dimensional terms are small. Our numerical analysis leads to the conclusion that these requirements are fulfilled in the regions shown below for the considered pentaquark states.

$$22.0 \text{ GeV}^2 \leq s_0 \leq 24.0 \text{ GeV}^2 \text{ } P_{c1} \text{ and } P_{c2} \text{ states,}$$

$$23.0 \text{ GeV}^2 \leq s_0 \leq 25.0 \text{ GeV}^2 \text{ for } P_{cs} \text{ state,}$$

$$5.0 \text{ GeV}^2 \leq M^2 \leq 7.0 \text{ GeV}^2 \text{ for } P_{c1} \text{ and } P_{c2} \text{ states,}$$

$$5.5 \text{ GeV}^2 \leq M^2 \leq 7.5 \text{ GeV}^2 \text{ for } P_{cs} \text{ state.}$$

By having the values of all input parameters, we can start carrying out numerical computations. In Fig. 1, as an example, we depict the dependencies of the magnetic dipole moments in diquark–diquark–antiquark picture on M^2 and s_0 . As is seen, the deviation of the results in connection with the s_0 is remarkable however there is much less dependence of the physical observables under consideration on the M^2 in its working window.

Our final results for the magnetic dipole moments are presented in Table 1. Our results cover errors originated from the uncertainty of the determinations of auxiliary parameters (M^2 and s_0) and other input parameters used in the analyses. The numerical values of the magnetic dipole moments acquired by means of two configurations differ considerably from each other, which can be used to determine the fundamental structure of these pentaquark states. That is to say, as many theoretical models give compatible results on the decay channels and spectroscopic parameters with the experimental data preventing us assigning precise substructure for pentaquarks, the experimental measurement of the magnetic dipole moments of these pentaquarks indeed can help us exactly distinguish their substructures. Since there are no theoretical result and experimental data for the results we obtained for these pentaquark states, we cannot compare our results. However, we may compare the result of the P_{cs} state with the $P_c(4312)$ state magnetic dipole moments. It can be seen that the quark configurations of the P_{cs} and $P_c(4312)$ particles are similar and therefore the magnetic

dipole moment results of these particles can be expected to be close to each other. In Ref. [59], the magnetic dipole moment of $P_c(4312)$ in the diquark–diquark–antiquark and molecular pictures are extracted as $\mu_{P_c} = 0.40 \pm 0.15 \mu_N$ and $\mu_{P_c} = 1.98 \pm 0.75 \mu_N$, respectively. The magnetic dipole moment of the $P_c(4312)$ pentaquark state has also been extracted via the QCD sum rule and its extension in the weak electromagnetic field by employing a molecular type interpolating current in Ref. [60]. The numerical value was obtained as $\mu_{P_c} = 0.59^{+10}_{-0.20}$. As one can see from these estimations, the numerical values for the magnetic dipole moments of $P_c(4312)$ and P_{cs} states acquired in the present study are close to each other and we see a reasonable SU(3) flavor violation which is roughly %15. The obtained results in both pictures are considerably different compared to the result of Ref. [60]. Comparing the results obtained using different theoretical models with our results can give an idea about the consistency of our predictions.

As a by product, we also obtain the electric quadrupole ($Q_{P_{c1}}$) and magnetic octupole ($O_{P_{c1}}$) moments of the P_{c1} pentaquark as

$$Q_{P_{c1}}^{Di} = (2.0^{+0.6}_{-0.5}) \times 10^{-2} \text{ fm}^2,$$

$$Q_{P_{c1}}^{Mol} = 0.28^{+0.09}_{-0.07} \text{ fm}^2, \tag{36}$$

$$O_{P_{c1}}^{Di} = (0.24^{+0.07}_{-0.06}) \times 10^{-3} \text{ fm}^3,$$

$$O_{P_{c1}}^{Mol} = (4.83^{+1.36}_{-1.13}) \times 10^{-3} \text{ fm}^3. \tag{37}$$

Just like the magnetic dipole moment results, we can see that the electric quadrupole and magnetic octupole moments results obtained by using two different pictures are different from each other. The $Q_{P_{c1}}$ and $O_{P_{c1}}$ of the P_{c1} pentaquark state showing a non-spherical charge distribution.

In summary, the observation of new pentaquark states such as $P_c(4312)$, $P_c(4440)$, $P_c(4457)$ and $P_{cs}(4459)$, ensures a new platform to investigate the exotic states in QCD. There are different interpretations of their inner structures and quantum numbers, and these should be shedded light on with further research. In the present work, stimulated by the observation of the hidden-charm pentaquark states we have achieved the magnetic dipole moments of the $P_c(4440)$, $P_c(4457)$ and $P_{cs}(4459)$ by considering them as diquark–diquark–antiquark and molecular pictures with quantum numbers $J^P = \frac{3}{2}^-$, $J^P = \frac{1}{2}^-$ and $J^P = \frac{1}{2}^-$ by means of the light-cone QCD sum rule, respectively. As a by product, the electric quadrupole and magnetic octupole moments of

the $P_c(4440)$ pentaquark have also extracted. Our predictions for electromagnetic multi-pole moments of pentaquark states may be checked via different theoretical models such as Lattice QCD, chiral perturbation theory etc. With the latest developments in the experimental side, we hope that we will be able to measure the magnetic dipole moment of newly formed multi-quark states, especially pentaquark states in the future. Any experimental measurements of the electromagnetic multi-pole moments of the hidden-charm pentaquark states and comparison of the obtained results with the predictions of the this study may provide as helpful knowledge on the internal structure of the these states as well as the non-perturbative behaviors of the strong interaction at the low-energy region.

Acknowledgements We thank Hua-Xing Chen for providing us the numeric value of the residue of the $P_{cs}(4459)$ state.

Data Availability Statement This manuscript has no associated data or the data will not be deposited. [Authors' comment: All the numerical and mathematical data have been included in the paper and we have no other data regarding this paper.]

Open Access This article is licensed under a Creative Commons Attribution 4.0 International License, which permits use, sharing, adaptation, distribution and reproduction in any medium or format, as long as you give appropriate credit to the original author(s) and the source, provide a link to the Creative Commons licence, and indicate if changes were made. The images or other third party material in this article are included in the article's Creative Commons licence, unless indicated otherwise in a credit line to the material. If material is not included in the article's Creative Commons licence and your intended use is not permitted by statutory regulation or exceeds the permitted use, you will need to obtain permission directly from the copyright holder. To view a copy of this licence, visit <http://creativecommons.org/licenses/by/4.0/>.
Funded by SCOAP³.

Appendix A: Explicit forms of the F_1^{Di} and F_2^{Di} functions

In this appendix, we give the explicit expressions for the F_1^{Di} and F_2^{Di} functions:

$$\begin{aligned}
 F_1^{Di} = & \frac{e \frac{m_{P_{c1}}^2}{M^2}}{\lambda_{P_{c1}}^{2-Di}} \left\{ \frac{\langle g_s^2 G^2 \rangle}{108716359680 \pi^7} \left[20 \pi^2 f_{3\gamma} \right. \right. \\
 & \times \left(4(32e_d + 41e_u) I[0, 4, 4, 0] \right. \\
 & + 3(9e_d + 20e_u) I[0, 4, 5, 0] \Big) I_2[\mathcal{V}] \\
 & + (72e_d + 720e_u - 702e_c) I[0, 5, 2, 1] \\
 & - (324e_d + 2184e_u - 2673e_c) I[0, 5, 2, 2] \\
 & + (492e_d + 2456e_u - 3511e_c) \\
 & \times I[0, 5, 2, 4] - (300e_d + 1240e_u - 1811e_c) I[0, 5, 2, 4] \\
 & + (60e_d + 248e_u - 271e_c) I[0, 5, 2, 5] \\
 & \left. \left. + (216e_d + 2160e_u \right. \right.
 \end{aligned}$$

$$\begin{aligned}
 & - 2106) I[0, 5, 3, 1] \\
 & + (684e_d + 4728e_d - 5693e_c) I[0, 5, 3, 2] \\
 & - (624e_d + 3424e_u - 4483e_c) I[0, 5, 3, 3] + (156e_d \\
 & + 856e_u - 893e_c) I[0, 5, 3, 4] \\
 & + (216e_d + 2160e_u - 2106e_c) I[0, 5, 4, 1] \\
 & - (396e_d + 2904e_u - 3375e_c) \\
 & \times I[0, 5, 4, 2] + (132e_d + 968e_u - 973e_c) I[0, 5, 4, 3] \\
 & - (72e_d + 720e_u - 702e_c) I[0, 5, 5, 1] + (36e_d + 360e_u \\
 & - 351e_c) I[0, 5, 5, 2] \Big] \\
 & - \frac{m_c \langle \bar{q}q \rangle}{3774873 \pi^5} \\
 & \times \left[192 e_c \left(I[0, 5, 2, 2] - 2 I[0, 5, 2, 3] \right. \right. \\
 & + I[0, 5, 2, 4] - 2 I[0, 5, 3, 2] \\
 & + 2 I[0, 5, 3, 3] + I[0, 5, 4, 2] \Big) \\
 & - 40 \pi^2 f_{3\gamma} (e_d + 10e_u) I_2[\mathcal{V}] I[0, 4, 4, 0] \\
 & + 3(e_d + 14e_u) I_4[\bar{S}] I[0, 5, 4, 0] \Big] \\
 & + \frac{f_{3\gamma}}{3019898880 \pi^5} (13e_d \\
 & + 58e_u) I_2[\mathcal{V}] I[0, 6, 5, 0] \\
 & - \frac{e_c}{880803840 \pi^7} \left[4 I[0, 7, 2, 3] \right. \\
 & - 13 I[0, 7, 2, 4] + 15 I[0, 7, 2, 5] \\
 & - 7 I[0, 7, 2, 6] + I[0, 7, 2, 7] - 12 I[0, 7, 3, 3] \\
 & + 27 I[0, 7, 3, 4] - 18 I[0, 7, 3, 5] + 3 I[0, 7, 3, 6] \\
 & + 12 I[0, 7, 4, 3] + 3 I[0, 7, 4, 5] \\
 & \left. \left. - 4 I[0, 7, 5, 3] + I[0, 7, 5, 4] \right] \right\}, \tag{38}
 \end{aligned}$$

$$\begin{aligned}
 F_2^{Di} = & \frac{m_{P_{c1}} e \frac{m_{P_{c1}}^2}{M^2}}{\lambda_{P_{c1}}^{2-Di}} \left\{ \frac{\langle g_s^2 G^2 \rangle}{108716359680 \pi^7} \left[20 f_{3\gamma} \pi^2 \right. \right. \\
 & \times \left\{ -4 \left((52e_d - 19e_u) I_2[\mathcal{A}] \right. \right. \\
 & - 9(32e_d + 41e_u) I_2[\mathcal{V}] + 4(3e_d + 2e_u) \\
 & \times I_6[\psi^v] \Big) I[0, 4, 4, 0] + 3 \left(8(-34e_d + e_u) I_2[\mathcal{A}] \right. \\
 & + 9(9e_d + 220e_u) I_2[\mathcal{V}] \Big) I[0, 4, 5, 0] \Big\} \\
 & - \left\{ (702e_c - 72e_d - 720e_u) \right. \\
 & \times I[0, 5, 2, 1] + (324e_d - 2673e_c \\
 & + 2184e_u) I[0, 5, 2, 2] + (-492e_d + 3511e_c \\
 & - 2456e_u) I[0, 5, 2, 3] + (300e_d \\
 & - 1811e_c + 1240e_u) I[0, 5, 2, 4] \\
 & + (-60e_d + 271e_c - 248e_u) I[0, 5, 2, 5] \\
 & + (216e_d - 2106e_c + 2160e_u) I[0, 5, 3, 1] \\
 & \left. \left. + (-684e_d + 5697e_c - 4728e_u) I[0, 5, 3, 2] \right. \right.
 \end{aligned}$$

$$\begin{aligned}
 & + (624e_d - 4484e_c + 3424e_u) I[0, 5, 3, 3] \\
 & + (893e_c - 156e_d - 856e_u) \\
 & \times I[0, 5, 3, 4] + (-216e_d + 2106e_c \\
 & - 2160e_u) I[0, 5, 4, 1] \\
 & + (396e_d - 3375e_c + 2904e_u) I[0, 5, 4, 2] + (-132e_d \\
 & + 973e_c - 968e_u) I[0, 5, 4, 3] \\
 & + (72e_d - 702e_c + 720e_u) I[0, 5, 5, 1] \\
 & + (-36e_d + 351e_c - 360e_u) I[0, 5, 5, 2] \Big] \\
 & - \frac{m_c \langle \bar{q}q \rangle}{125829120 \pi^5} \\
 & \times \left[-120 (e_d + 10e_u) f_{3\gamma} \pi^2 I_2[\mathcal{V}] I[0, 4, 4, 0] \right. \\
 & + (3e_d + 14e_u) I_4[\mathcal{S}] + 2e_d I_4[\mathcal{T}_1] I[0, 5, 4, 0] \\
 & + 64e_c \left(I[0, 5, 2, 2] - 2 I[0, 5, 2, 3] \right. \\
 & + I[0, 5, 2, 4] - 2 I[0, 5, 3, 2] \\
 & \left. + 2 I[0, 5, 3, 3] + I[0, 5, 4, 2] \right) \Big] \\
 & + \frac{f_{3\gamma}}{3019898880 \pi^5} (13e_d + 58e_u) I_2[\mathcal{V}] I[0, 6, 5, 0] \\
 & - \frac{e_c}{880803840 \pi^7} \left[4 I[0, 7, 2, 3] \right. \\
 & - 13 I[0, 7, 2, 4] + 15 I[0, 7, 2, 5] - 7 I[0, 7, 2, 6] \\
 & + I[0, 7, 2, 7] - 12 I[0, 7, 3, 3] \\
 & + 27 I[0, 7, 3, 4] - 18 I[0, 7, 3, 5] \\
 & + 3 I[0, 7, 3, 6] + 12 I[0, 7, 4, 3] \\
 & - 15 I[0, 7, 4, 4] + 3 I[0, 7, 4, 5] - 4 I[0, 7, 5, 3] \\
 & \left. + I[0, 7, 5, 4] \right]. \tag{39}
 \end{aligned}$$

We should also point out that in the above expressions, for simplicity we have only given the terms that give important contributions to the numerical values of the magnetic moments, and have not presented many higher dimensional contributions, although they have been considered in the numerical calculations.

The functions $I[n, m, l, k]$, $I_1[\mathcal{A}]$, $I_2[\mathcal{A}]$, $I_3[\mathcal{A}]$, $I_4[\mathcal{A}]$, $I_5[\mathcal{A}]$, and $I_6[\mathcal{A}]$ are defined as:

$$\begin{aligned}
 I[n, m, l, k] &= \int_{4m_c^2}^{s_0} ds \int_0^1 dt \int_0^1 dw e^{-s/M^2} s^n (s - 4m_c^2)^m t^l w^k, \\
 I_1[\mathcal{A}] &= \int D\alpha_i \int_0^1 dv \mathcal{A}(\alpha_{\bar{q}}, \alpha_q, \alpha_g) \delta'(\alpha_q + \bar{v}\alpha_g - u_0), \\
 I_2[\mathcal{A}] &= \int D\alpha_i \int_0^1 dv \mathcal{A}(\alpha_{\bar{q}}, \alpha_q, \alpha_g) \delta'(\alpha_{\bar{q}} + v\alpha_g - u_0), \\
 I_3[\mathcal{A}] &= \int D\alpha_i \int_0^1 dv \mathcal{A}(\alpha_{\bar{q}}, \alpha_q, \alpha_g) \delta(\alpha_q + \bar{v}\alpha_g - u_0), \\
 I_4[\mathcal{A}] &= \int D\alpha_i \int_0^1 dv \mathcal{A}(\alpha_{\bar{q}}, \alpha_q, \alpha_g) \delta(\alpha_{\bar{q}} + v\alpha_g - u_0),
 \end{aligned}$$

$$\begin{aligned}
 I_5[\mathcal{A}] &= \int_0^1 du A(u) \delta'(u - u_0), \\
 I_6[\mathcal{A}] &= \int_0^1 du A(u),
 \end{aligned}$$

where \mathcal{A} represents the corresponding photon distribution amplitudes.

References

1. H.-X. Chen, W. Chen, X. Liu, S.-L. Zhu, The hidden-charm pentaquark and tetraquark states. *Phys. Rep.* **639**, 1–121 (2016). <https://doi.org/10.1016/j.physrep.2016.05.004>. arXiv:1601.02092
2. A. Ali, J.S. Lange, S. Stone, Exotics: heavy pentaquarks and tetraquarks. *Prog. Part. Nucl. Phys.* **97**, 123–198 (2017). <https://doi.org/10.1016/j.pnpnp.2017.08.003>. arXiv:1706.00610
3. A. Esposito, A. Pilloni, A.D. Polosa, Multiquark resonances. *Phys. Rep.* **668**, 1–97 (2017). <https://doi.org/10.1016/j.physrep.2016.11.002>. arXiv:1611.07920
4. S.L. Olsen, T. Skwarnicki, D. Zieminska, Nonstandard heavy mesons and baryons: experimental evidence. *Rev. Mod. Phys.* **90**(1), 015003 (2018). <https://doi.org/10.1103/RevModPhys.90.015003>. arXiv:1708.04012
5. R.F. Lebed, R.E. Mitchell, E.S. Swanson, Heavy-quark QCD exotica. *Prog. Part. Nucl. Phys.* **93**, 143–194 (2017). <https://doi.org/10.1016/j.pnpnp.2016.11.003>. arXiv:1610.04528
6. F.-K. Guo, C. Hanhart, U.-G. Meißner, Q. Wang, Q. Zhao, B.-S. Zou, Hadronic molecules. *Rev. Mod. Phys.* **90**(1), 015004 (2018). <https://doi.org/10.1103/RevModPhys.90.015004>. arXiv:1705.00141
7. R.M. Albuquerque, J.M. Dias, K.P. Khemchandani, A. Martínez Torres, F.S. Navarra, M. Nielsen, C.M. Zanetti, QCD sum rules approach to the X , Y and Z states. *J. Phys. G* **46**(9), 093002 (2019). <https://doi.org/10.1088/1361-6471/ab2678>. arXiv:1812.08207
8. N. Brambilla, S. Eidelman, C. Hanhart, A. Nefediev, C.-P. Shen, C.E. Thomas, A. Vairo, C.-Z. Yuan, The XYZ states: experimental and theoretical status and perspectives. *Phys. Rep.* **873**, 1–154 (2020). <https://doi.org/10.1016/j.physrep.2020.05.001>. arXiv:1907.07583
9. Y.-R. Liu, H.-X. Chen, W. Chen, X. Liu, S.-L. Zhu, Pentaquark and tetraquark states. *Prog. Part. Nucl. Phys.* **107**, 237–320 (2019). <https://doi.org/10.1016/j.pnpnp.2019.04.003>. arXiv:1903.11976
10. S. Agaev, K. Azizi, H. Sundu, Four-quark exotic mesons. *Turk. J. Phys.* **44**(2), 95–173 (2020). <https://doi.org/10.3906/fiz-2003-15>. arXiv:2004.12079
11. X.-K. Dong, F.-K. Guo, B.-S. Zou, A survey of heavy-antiheavy hadronic molecules. *Progr. Phys.* **41**, 65–93 (2021). <https://doi.org/10.13725/j.cnki.pip.2021.02.001>. arXiv:2101.01021
12. R. Aaij et al., Observation of a narrow pentaquark state, $P_c(4312)^+$, and of two-peak structure of the $P_c(4450)^+$. *Phys. Rev. Lett.* **122**(22), 222001 (2019). <https://doi.org/10.1103/PhysRevLett.122.222001>. arXiv:1904.03947
13. R. Aaij, et al., Evidence of a $J/\psi \Lambda$ structure and observation of excited \mathcal{E}^- states in the $\mathcal{E}_b^- \rightarrow J/\psi^-$ decay (2020). arXiv:2012.10380
14. R. Chen, Z.-F. Sun, X. Liu, S.-L. Zhu, Strong LHCb evidence supporting the existence of the hidden-charm molecular pentaquarks. *Phys. Rev. D* **100**(1), 011502 (2019). <https://doi.org/10.1103/PhysRevD.100.011502>. arXiv:1903.11013
15. H.-X. Chen, W. Chen, S.-L. Zhu, Possible interpretations of the $P_c(4312)$, $P_c(4440)$, and $P_c(4457)$. *Phys. Rev. D* **100**(5), 051501 (2019). <https://doi.org/10.1103/PhysRevD.100.051501>. arXiv:1903.11001

16. M.-Z. Liu, Y.-W. Pan, F.-Z. Peng, M.S. Sánchez, L.-S. Geng, A. Hosaka, M.P. Valderrama, Emergence of a complete heavy-quark spin symmetry multiplet: seven molecular pentaquarks in light of the latest LHCb analysis. *Phys. Rev. Lett.* **122**(24), 242001 (2019). <https://doi.org/10.1103/PhysRevLett.122.242001>. [arXiv:1903.11560](https://arxiv.org/abs/1903.11560)
17. J. He, Study of $P_c(4457)$, $P_c(4440)$, and $P_c(4312)$ in a quasipotential Bethe–Salpeter equation approach. *Eur. Phys. J. C* **79**(5), 393 (2019). <https://doi.org/10.1140/epjc/s10052-019-6906-1>. [arXiv:1903.11872](https://arxiv.org/abs/1903.11872)
18. C.-J. Xiao, Y. Huang, Y.-B. Dong, L.-S. Geng, D.-Y. Chen, Exploring the molecular scenario of $P_c(4312)$, $P_c(4440)$, and $P_c(4457)$. *Phys. Rev. D* **100**(1), 014022 (2019). <https://doi.org/10.1103/PhysRevD.100.014022>. [arXiv:1904.00872](https://arxiv.org/abs/1904.00872)
19. Z.-H. Guo, J.A. Oller, Anatomy of the newly observed hidden-charm pentaquark states: $P_c(4312)$, $P_c(4440)$ and $P_c(4457)$. *Phys. Lett. B* **793**, 144–149 (2019). <https://doi.org/10.1016/j.physletb.2019.04.053>. [arXiv:1904.00851](https://arxiv.org/abs/1904.00851)
20. C.W. Xiao, J. Nieves, E. Oset, Heavy quark spin symmetric molecular states from $\bar{D}^{(*)}\Sigma_c^{(*)}$ and other coupled channels in the light of the recent LHCb pentaquarks. *Phys. Rev. D* **100**(1), 014021 (2019). <https://doi.org/10.1103/PhysRevD.100.014021>. [arXiv:1904.01296](https://arxiv.org/abs/1904.01296)
21. J.-R. Zhang, Exploring a $\Sigma_c \bar{D}$ state: with focus on $P_c(4312)^+$. *Eur. Phys. J. C* **79**(12), 1001 (2019). <https://doi.org/10.1140/epjc/s10052-019-7529-2>. [arXiv:1904.10711](https://arxiv.org/abs/1904.10711)
22. Q. Wu, D.-Y. Chen, Production of P_c states from Λ_b decay. *Phys. Rev. D* **100**(11), 114002 (2019). <https://doi.org/10.1103/PhysRevD.100.114002>. [arXiv:1906.02480](https://arxiv.org/abs/1906.02480)
23. B. Wang, L. Meng, S.-L. Zhu, Hidden-charm and hidden-bottom molecular pentaquarks in chiral effective field theory. *JHEP* **11**, 108 (2019). [https://doi.org/10.1007/JHEP11\(2019\)108](https://doi.org/10.1007/JHEP11(2019)108). [arXiv:1909.13054](https://arxiv.org/abs/1909.13054)
24. H. Xu, Q. Li, C.-H. Chang, G.-L. Wang, Recently observed P_c as molecular states and possible mixture of $P_c(4457)$. *Phys. Rev. D* **101**(5), 054037 (2020). <https://doi.org/10.1103/PhysRevD.101.054037>. [arXiv:2001.02980](https://arxiv.org/abs/2001.02980)
25. F.-Z. Peng, J.-X. Lu, M.S. Sánchez, M.-J. Yan, M.P. Valderrama, Peaks within peaks and the possible two-peak structure of the $P_c(4457)$: the effective field theory perspective. *Phys. Rev. D* **103**(1), 014023 (2021). <https://doi.org/10.1103/PhysRevD.103.014023>. [arXiv:2007.01198](https://arxiv.org/abs/2007.01198)
26. Y. Shimizu, Y. Yamaguchi, M. Harada, Heavy quark spin multiplet structure of $P_c(4312)$, $P_c(4440)$, and $P_c(4457)$ (2019). [arXiv:1904.00587](https://arxiv.org/abs/1904.00587)
27. R. Zhu, X. Liu, H. Huang, C.-F. Qiao, Analyzing doubly heavy tetra- and penta-quark states by variational method. *Phys. Lett. B* **797**, 134869 (2019). <https://doi.org/10.1016/j.physletb.2019.134869>. [arXiv:1904.10285](https://arxiv.org/abs/1904.10285)
28. Z.-G. Wang, Analysis of the $P_c(4312)$, $P_c(4440)$, $P_c(4457)$ and related hidden-charm pentaquark states with QCD sum rules. *Int. J. Mod. Phys. A* **35**(01), 2050003 (2020). <https://doi.org/10.1142/S0217751X20500037>. [arXiv:1905.02892](https://arxiv.org/abs/1905.02892)
29. Z.-G. Wang, Analysis of the $\bar{D}\Sigma_c$, $\bar{D}\Sigma_c^*$, $\bar{D}^*\Sigma_c$ and $\bar{D}^*\Sigma_c^*$ pentaquark molecular states with QCD sum rules. *Int. J. Mod. Phys. A* **34**(19), 1950097 (2019). <https://doi.org/10.1142/S0217751X19500970>. [arXiv:1806.10384](https://arxiv.org/abs/1806.10384)
30. J.-B. Cheng, Y.-R. Liu, $P_c(4457)^+$, $P_c(4440)^+$, and $P_c(4312)^+$: molecules or compact pentaquarks? *Phys. Rev. D* **100**(5), 054002 (2019). <https://doi.org/10.1103/PhysRevD.100.054002>. [arXiv:1905.08605](https://arxiv.org/abs/1905.08605)
31. Y. Yamaguchi, H. García-Tecocoatzí, A. Giachino, A. Hosaka, E. Santopinto, S. Takeuchi, M. Takizawa, P_c pentaquarks with chiral tensor and quark dynamics. *Phys. Rev. D* **101**(9), 091502 (2020). <https://doi.org/10.1103/PhysRevD.101.091502>. [arXiv:1907.04684](https://arxiv.org/abs/1907.04684)
32. Y.-W. Pan, M.-Z. Liu, F.-Z. Peng, M.S. Sánchez, L.-S. Geng, M.P. Valderrama, Model independent determination of the spins of the $P_c(4440)$ and $P_c(4457)$ from the spectroscopy of the triply charmed dibaryons. *Phys. Rev. D* **102**(1), 011504 (2020). <https://doi.org/10.1103/PhysRevD.102.011504>. [arXiv:1907.11220](https://arxiv.org/abs/1907.11220)
33. M.-Z. Liu, T.-W. Wu, M.S. Sánchez, M.P. Valderrama, L.-S. Geng, J.-J. Xie, Spin-parities of the $P_c(4440)$ and $P_c(4457)$ in the one-boson-exchange model. *Phys. Rev. D* **103**(5), 054004 (2021). <https://doi.org/10.1103/PhysRevD.103.054004>. [arXiv:1907.06093](https://arxiv.org/abs/1907.06093)
34. C. Fernández-Ramírez, A. Pilloni, M. Albaladejo, A. Jackura, V. Mathieu, M. Mikhasenko, J.A. Silva-Castro, A.P. Szczepaniak, Interpretation of the LHCb $P_c(4312)^+$ Signal. *Phys. Rev. Lett.* **123**(9), 092001 (2019). <https://doi.org/10.1103/PhysRevLett.123.092001>. [arXiv:1904.10021](https://arxiv.org/abs/1904.10021)
35. M.I. Eides, V.Y. Petrov, M.V. Polyakov, New LHCb pentaquarks as hadrocharmonium states. *Mod. Phys. Lett. A* **35**(18), 2050151 (2020). <https://doi.org/10.1142/S0217732320501515>. [arXiv:1904.11616](https://arxiv.org/abs/1904.11616)
36. F.-K. Guo, H.-J. Jing, U.-G. Meißner, S. Sakai, Isospin breaking decays as a diagnosis of the hadronic molecular structure of the $P_c(4457)$. *Phys. Rev. D* **99**(9), 091501 (2019). <https://doi.org/10.1103/PhysRevD.99.091501>. [arXiv:1903.11503](https://arxiv.org/abs/1903.11503)
37. X. Cao, J.-P. Dai, Confronting pentaquark photoproduction with new LHCb observations. *Phys. Rev. D* **100**(5), 054033 (2019). <https://doi.org/10.1103/PhysRevD.100.054033>. [arXiv:1904.06015](https://arxiv.org/abs/1904.06015)
38. X.-Y. Wang, J. He, X.-R. Chen, Q. Wang, X. Zhu, Pion-induced production of hidden-charm pentaquarks $P_c(4312)$, $P_c(4440)$, and $P_c(4457)$. *Phys. Lett. B* **797**, 134862 (2019). <https://doi.org/10.1016/j.physletb.2019.134862>. [arXiv:1906.04044](https://arxiv.org/abs/1906.04044)
39. X.-Y. Wang, X.-R. Chen, J. He, Possibility to study pentaquark states $P_c(4312)$, $P_c(4440)$, and $P_c(4457)$ in $\gamma p \rightarrow J/\psi p$ reaction. *Phys. Rev. D* **99**(11), 114007 (2019). <https://doi.org/10.1103/PhysRevD.99.114007>. [arXiv:1904.11706](https://arxiv.org/abs/1904.11706)
40. C.W. Xiao, J.X. Lu, J.J. Wu, L.S. Geng, How to reveal the nature of three or more pentaquark states. *Phys. Rev. D* **102**(5), 056018 (2020). <https://doi.org/10.1103/PhysRevD.102.056018>. [arXiv:2007.12106](https://arxiv.org/abs/2007.12106)
41. H. Mutuk, Neural network study of hidden-charm pentaquark resonances. *Chin. Phys. C* **43**(9), 093103 (2019). <https://doi.org/10.1088/1674-1137/43/9/093103>. [arXiv:1904.09756](https://arxiv.org/abs/1904.09756)
42. G. Yang, J. Ping, J. Segovia, Doubly charmed pentaquarks. *Phys. Rev. D* **101**(7), 074030 (2020). <https://doi.org/10.1103/PhysRevD.101.074030>. [arXiv:2003.05253](https://arxiv.org/abs/2003.05253)
43. Y. Dong, P. Shen, F. Huang, Z. Zhang, Selected strong decays of pentaquark state $P_c(4312)$ in a chiral constituent quark model. *Eur. Phys. J. C* **80**(4), 341 (2020). <https://doi.org/10.1140/epjc/s10052-020-7890-1>. [arXiv:2002.08051](https://arxiv.org/abs/2002.08051)
44. Z.-G. Wang, H.-J. Wang, Q. Xin, The hadronic coupling constants of the lowest hidden-charm pentaquark state with the QCD sum rules in solid quark-hadron duality (2020). [arXiv:2005.00535](https://arxiv.org/abs/2005.00535)
45. M.-L. Du, V. Baru, F.-K. Guo, C. Hanhart, U.-G. Meißner, J.A. Oller, Q. Wang, Interpretation of the LHCb P_c states as hadronic molecules and hints of a narrow $P_c(4380)$. *Phys. Rev. Lett.* **124**(7), 072001 (2020). <https://doi.org/10.1103/PhysRevLett.124.072001>. [arXiv:1910.11846](https://arxiv.org/abs/1910.11846)
46. G.-J. Wang, L.-Y. Xiao, R. Chen, X.-H. Liu, X. Liu, S.-L. Zhu, Probing hidden-charm decay properties of P_c states in a molecular scenario. *Phys. Rev. D* **102**(3), 036012 (2020). <https://doi.org/10.1103/PhysRevD.102.036012>. [arXiv:1911.09613](https://arxiv.org/abs/1911.09613)
47. K. Azizi, Y. Sarac, H. Sundu, Properties of $P_c(4312)$ pentaquark (2020). [arXiv:2011.05828](https://arxiv.org/abs/2011.05828)

48. H.-X. Chen, Hidden-charm pentaquark states through the current algebra: from their productions to decays (2020). [arXiv:2011.07187](https://arxiv.org/abs/2011.07187)
49. H.-X. Chen, W. Chen, X. Liu, X.-H. Liu, Establishing the first hidden-charm pentaquark with strangeness (2020). [arXiv:2011.01079](https://arxiv.org/abs/2011.01079)
50. M.-Z. Liu, Y.-W. Pan, L.-S. Geng, Can discovery of hidden charm strange pentaquark states help determine the spins of $P_c(4440)$ and $P_c(4457)$? *Phys. Rev. D* **103**(3), 034003 (2021). <https://doi.org/10.1103/PhysRevD.103.034003>. [arXiv:2011.07935](https://arxiv.org/abs/2011.07935)
51. F.-Z. Peng, M.-J. Yan, M.S. Sánchez, M.P. Valderrama, The $P_{cs}(4459)$ pentaquark from a combined effective field theory and phenomenological perspectives (2020). [arXiv:2011.01915](https://arxiv.org/abs/2011.01915)
52. R. Chen, Can the newly reported $P_{cs}(4459)$ be a strange hidden-charm $\Xi_c \bar{D}^*$ molecular pentaquark? *Phys. Rev. D* **103**(5), 054007 (2021). <https://doi.org/10.1103/PhysRevD.103.054007>. [arXiv:2011.07214](https://arxiv.org/abs/2011.07214)
53. Z.-G. Wang, Analysis of the $P_{cs}(4459)$ as the hidden-charm pentaquark state with QCD sum rules (2020). [arXiv:2011.05102](https://arxiv.org/abs/2011.05102)
54. K. Azizi, Y. Sarac, H. Sundu, Investigation of $P_{cs}(4459)^0$ pentaquark via its strong decay to $\Lambda J/\Psi$ (2021). [arXiv:2101.07850](https://arxiv.org/abs/2101.07850)
55. J.-T. Zhu, L.-Q. Song, J. He, $P_{cs}(4459)$ and other possible molecular states from $\Xi_c^{(*)} \bar{D}^{(*)}$ and $\Xi_c' \bar{D}^{(*)}$ interactions (2021). [arXiv:2101.12441](https://arxiv.org/abs/2101.12441)
56. G.-J. Wang, R. Chen, L. Ma, X. Liu, S.-L. Zhu, Magnetic moments of the hidden-charm pentaquark states. *Phys. Rev. D* **94**(9), 094018 (2016). <https://doi.org/10.1103/PhysRevD.94.094018>. [arXiv:1605.01337](https://arxiv.org/abs/1605.01337)
57. U. Özdem, K. Azizi, Electromagnetic multipole moments of the $P_c^+(4380)$ pentaquark in light-cone QCD. *Eur. Phys. J. C* **78**(5), 379 (2018). <https://doi.org/10.1140/epjc/s10052-018-5873-2>. [arXiv:1803.06831](https://arxiv.org/abs/1803.06831)
58. E. Ortiz-Pacheco, R. Bijker, C. Fernández-Ramírez, Hidden charm pentaquarks: mass spectrum, magnetic moments, and photocouplings. *J. Phys. G* **46**(6), 065104 (2019). <https://doi.org/10.1088/1361-6471/ab096d>. [arXiv:1808.10512](https://arxiv.org/abs/1808.10512)
59. U. Özdem, Electromagnetic properties of the $P_c(4312)$ pentaquark state. *Chin. Phys. C* **45**(2), 023119 (2021). <https://doi.org/10.1088/1674-1137/abd01c>
60. Y.-J. Xu, Y.-L. Liu, M.-Q. Huang, The magnetic moment of $P_c(4312)$ as a $\bar{D}\Sigma_c$ molecular state (2020). [arXiv:2008.07937](https://arxiv.org/abs/2008.07937)
61. V.L. Chernyak, I.R. Zhitnitsky, B meson exclusive decays into baryons. *Nucl. Phys. B* **345**, 137–172 (1990). [https://doi.org/10.1016/0550-3213\(90\)90612-H](https://doi.org/10.1016/0550-3213(90)90612-H)
62. V.M. Braun, I.E. Filyanov, QCD sum rules in exclusive kinematics and pion wave function. *Sov. J. Nucl. Phys.* **50**, 511 (1989). <https://doi.org/10.1007/BF01548594>
63. I.I. Balitsky, V.M. Braun, A.V. Kolesnichenko, Radiative decay $\sigma + \rightarrow p \gamma$ in quantum chromodynamics. *Nucl. Phys. B* **312**, 509–550 (1989). [https://doi.org/10.1016/0550-3213\(89\)90570-1](https://doi.org/10.1016/0550-3213(89)90570-1)
64. I.I. Balitsky, V.M. Braun, Evolution equations for QCD string operators. *Nucl. Phys. B* **311**, 541–584 (1989). [https://doi.org/10.1016/0550-3213\(89\)90168-5](https://doi.org/10.1016/0550-3213(89)90168-5)
65. H.J. Weber, H. Arenhovel, Isobar configurations in nuclei. *Phys. Rep.* **36**, 277–348 (1978). [https://doi.org/10.1016/0370-1573\(78\)90187-4](https://doi.org/10.1016/0370-1573(78)90187-4)
66. S. Nozawa, D.B. Leinweber, Electromagnetic form-factors of spin 3/2 baryons. *Phys. Rev. D* **42**, 3567–3571 (1990). <https://doi.org/10.1103/PhysRevD.42.3567>
67. V. Pascalutsa, M. Vanderhaeghen, S.N. Yang, Electromagnetic excitation of the Delta(1232)-resonance. *Phys. Rep.* **437**, 125–232 (2007). <https://doi.org/10.1016/j.physrep.2006.09.006>. [arXiv:hep-ph/0609004](https://arxiv.org/abs/hep-ph/0609004)
68. G. Ramalho, M.T. Pena, F. Gross, Electric quadrupole and magnetic octupole moments of the Delta. *Phys. Lett. B* **678**, 355–358 (2009). <https://doi.org/10.1016/j.physletb.2009.06.052>. [arXiv:0902.4212](https://arxiv.org/abs/0902.4212)
69. V.M. Belyaev, B.L. Ioffe, Determination of the baryon mass and baryon resonances from the quantum-chromodynamics sum rule. Strange baryons. *Sov. Phys. JETP* **57**, 716–721 (1983)
70. C. Patrignani et al., Review of particle physics. *Chin. Phys. C* **40**(10), 100001 (2016). <https://doi.org/10.1088/1674-1137/40/10/100001>
71. P. Ball, V.M. Braun, N. Kivel, Photon distribution amplitudes in QCD. *Nucl. Phys. B* **649**, 263–296 (2003). [https://doi.org/10.1016/S0550-3213\(02\)01017-9](https://doi.org/10.1016/S0550-3213(02)01017-9). [arXiv:hep-ph/0207307](https://arxiv.org/abs/hep-ph/0207307)
72. B.L. Ioffe, QCD at low energies. *Prog. Part. Nucl. Phys.* **56**, 232–277 (2006). <https://doi.org/10.1016/j.pnpnp.2005.05.001>. [arXiv:hep-ph/0502148](https://arxiv.org/abs/hep-ph/0502148)
73. M. Nielsen, F.S. Navarra, S.H. Lee, New charmonium states in QCD sum rules: a concise review. *Phys. Rep.* **497**, 41–83 (2010). <https://doi.org/10.1016/j.physrep.2010.07.005>. [arXiv:0911.1958](https://arxiv.org/abs/0911.1958)